INTERNATIONAL JOURNAL OF GEOMAGNETISM AND AERONOMY
VOL. 6, GI2002, doi:10.1029/2004GI000092, 2006

# Localization of the source of ionospheric disturbance generated during an earthquake

E. L. Afraimovich, E. I. Astafieva, and V. V. Kirushkin

Institute of Solar-Terrestrial Physics, Irkutsk, Russia

Received 2 December 2004; revised 6 September 2005; accepted 4 October 2005; published 20 January 2006.

[1] For the first time a method is developed of localization of the source and determination of the characteristics of wave disturbances generated during earthquakes. In the method the disturbances in the total electron content registered at the GPS receiver network are considered as a set of signals of a nonequidistant phased grating of "ionospheric detectors" with known coordinates. As a result of solution of the equation system for the plane and spherical front relative to the measured parameters of the disturbance, the phase velocity of the wave disturbance and also the position and time of switching on of the source are determined. It is found that the ionospheric disturbances generated during strong earthquakes have the form of a spherical wave diverging with a velocity of $\sim$1000 m s$^{-1}$ from the "secondary" source localized over the epicenter at the level of the maximum of the ionospheric $F2$ layer (300–400 km), the time of the source "switching off" delaying relatively the main seismic shock by about 10 min. These results agree to the theoretical models according to which the atmospheric disturbance propagates in a narrow cone of zenith angles up to ionospheric heights and then diverges in the form of a spherical wave with a radial velocity close to the speed of sound at these altitudes. *INDEX TERMS:* 7215 Seismology: Earthquake source observations; 7851 Space Plasma Physics: Shock waves; 2439 Ionosphere: Ionospheric irregularities; *KEYWORDS:* Earthquake; Acoustic gravity waves; Ionospheric irregularities.

**Citation:** Afraimovich, E. L., E. I. Astafieva, and V. V. Kirushkin (2006), Localization of the source of ionospheric disturbance generated during an earthquake, *Int. J. Geomagn. Aeron., 6,* GI2002, doi:10.1029/2004GI000092.

## 1. Introduction

[2] Many papers have been dedicated to studies of the ionospheric response to disturbances generated at the pulse impact on the terrestrial atmosphere [*Ahmadov and Kunitsyn,* 2003, 2004; *Calais and Minster*, 1995; *Golitsyn and Klyatskin,* 1967; *Orlov and Uralov*, 1984; *Pavlov*, 1986; *Row,* 1967; *Rudenko and Uralov*, 1995]. Nuclear tests, industrial explosions, and large earthquakes may be considered as sources of such impacts. The shift of the Earth surface leads to generation of acoustic gravity waves (AGW) propagating in the atmosphere with an increase of the amplitude up to high altitudes where they are able to initiate the plasma motion due to the collision interaction of neutral and charged particles.

[3] The ionospheric irregularity influences significantly the evolution of the acoustic wave. At the upward propagation there occurs an increase of the wave amplitude and in the case of weak dissipation nonlinear effects appear [*Pavlov*, 1986]. A shock wave is formed and at the accent its profile gets a triangle shape [*Uizem*, 1977].

[4] The specific mechanism of formation of such disturbances is not yet clear. There are a few models explaining ionospheric disturbances: generation of infrasonic waves [*Calais et al.*, 1998], generation of IGW [*Francis*, 1975], eddy motions of the neural atmospheric constituents excited after a passage of the acoustic pulse [*Andreeva et al.*, 2001], generation of shock-acoustic waves (SAW) [*Afraimovich et al.,* 2001a, 2001b; *Nagorsky and Taraschuk*, 1992], and so on. Various terms different by physical interpretation are used in the publications for the ionospheric response of the shock wave including the term shock-acoustic wave [*Nagorsky*, 1985; *Nagorsky and Taraschuk*, 1992]. For the sake of convenience in this paper we will use this term as well as the more general term "ionospheric disturbance" (ID).

[5] The approach to solution of the problem of ionospheric disturbance generation during earthquakes is present even in early publications and includes a substitution of the epicenter emitter by a ground-based point source of velocity or by an explosion. The substitution of the earthquake zone by a point source is fruitful describing long-period AGW at


1524–4423/06/2004GI000092$18.00

very long (thousands of km) distances from the epicenter [*Row*, 1967]. Visual similarity of ionospheric disturbances at small (hundreds of km) distances from the epicenter to disturbances from ground-based explosions was discussed by *Calais et al.* [1998].

[6] *Barry et al.* [1966] showed that according to the theory of the linear acoustics a large ground-based surface explosion is able to generate a pressure wave with the amplitude reaching a few percents of the background atmospheric pressure at a height of 200 km over the explosion epicenter. The analysis of the interaction of this wave to the ionosphere makes it possible to assume that such a wave can be detected by the ionospheric diagnosis methods. Measurements conducted in July 1964 by a high-quality vertical sounding during the 500-t explosion (Suffield, Alberta, Canada) confirmed this hypothesis. The amplitude and duration of the detected phase disturbances were 100 rad and 2 min, respectively, the disturbance phase corresponding to the modeling results for the acoustic wave.

[7] *Fitzgerald* [1997] 565 s after the surface explosion in New Mexico with the efficient energy of 2 kt ($8.5 \times 10^{12}$ J) detected by the method of the GPS monitoring of the total electron content (TEC) a disturbance with an amplitude of 0.14 TECU ($10^{16}$ el m$^{-2}$) and duration of 80 s. The acoustic disturbance needed to produce such ionospheric disturbance is well modeled as an N wave with the spatial dimensions and relative amplitude of 35 km and 12%, respectively, propagating with a radial velocity 700 m s$^{-1}$. Similar results concerning the ionospheric response of this explosion have been earlier obtained registering TEC by the measurements of rotation of the polarization plane of the signal from the geostationary satellite GOES [*Massey et al.*, 1994].

[8] During conducting three powerful explosions in eastern Wyoming (United States) in July and August 1996 five GPS receivers were installed [*Calais et al.*, 1998]. Ionospheric disturbances what began 10–15 min after the explosion and lasted about 30 min propagating with a horizontal velocity of 1200 m s$^{-1}$ were registered. These irregularities were interpreted as disturbances formed by the direct acoustic wave generated by the explosion.

[9] Using the GPS receivers, *Calais and Minster* [1995] 10–30 min after the earthquake in California on 17 January 1994 (with a magnitude of 6.7) observed in the time series of TEC anomalous signal in the period range 3–10 min. The frequency and propagation phase velocity (300–600 m s$^{-1}$) agree to the results of numerical simulation for atmospheric AGW caused by a strong shift of the Earth surface during the earthquake.

[10] It should be noted that despite the above mentioned similarity in ionospheric disturbances caused by industrial ground-based and underground nuclear explosions, the generation mechanisms are principally different [*Rudenko and Uralov*, 1995]. The Earth surface disturbed by the explosion is a source of emission at an underground nuclear test as well as at an earthquake. The intensity and spectral composition of the generated acoustic signal demonstrate (unlike a surface explosion) a strong dependence on the zenith angle and are completely determined by the form, dimensions, and characteristics of the Earth surface motion in the epicenter of the underground explosion zone. The width of the "directivity diagram" of the acoustic signal propagating from the disturbed Earth surface is very narrow: $\Delta\theta \leq 5^\circ$. The shape and duration of the signal depend strongly on the zenith angle $\theta$ of the acoustic ray from the epicenter [*Rudenko and Uralov*, 1995].

[11] The scheme of formation and propagation of an ionospheric disturbance from a swallow underground source was presented by *Rudenko and Uralov* [1995]. The underground point of explosion $\varepsilon$ generates a spherical elastic wave in the rocks. Its appearance on the Earth surface ($z = 0$) one can compare to a strong shock. As a result the rock pieces A–G are "separated" [*Rodionov et al.*, 1971], then slightly lifted and then return to the initial position. This process is accompanied by generation in the atmosphere of an acoustic wave. Because of strong nonlinearity of the characteristics (parameters) of the air near the "lithosphere-atmosphere" boundary high-frequency seismic signals may generate air streams inducing low-frequency waves in the atmosphere. The nonlinear flow plays the role of an energetic connection between the high-frequency seismic motions and low-frequency atmospheric waves.

[12] In some papers [*Ahmadov and Kunitsyn*, 2003, 2004; *Pavlov*, 1979, 1986; *Row*, 1967] a grounding of the model is presented. In this model the ionospheric response to an earthquake is caused by a wave disturbance from the secondary source located not in the epicenter but at ionospheric heights over the epicenter. However, no confirmation of such mechanism has been presented in publications.

[13] Currently, the principal time parameters characterizing ionospheric response to SAW (shape, amplitude, and period) are studied fairly well. In publications, there is a strong scatter of the data on the main parameters of SAW generated during earthquakes. The oscillation period and propagation velocity of the ionospheric response to SAW vary from 30 to 300 s and from 700 to 1200 m s$^{-1}$, respectively [*Afraimovich et al.*, 1984; *Blanc and Jacobson*, 1989; *Calais et al.*, 1998; *Fitzgerald,* 1997]. Determination of spatial-time characteristics of ionospheric disturbances (ID) still stays an actual problem. This problem includes a wide set of tasks, in particular: calculation of the phase and group velocity of ID, determination of the direction of its propagation and location of the disturbance source, and also a wider problem of studying of the shape and dynamics of the SAW front propagation.

[14] The absence of complete and reliable data on the SAW parameters is due mainly to the defects of the existing radiophysical methods and detection means. The main amount of the data has been obtained by measurements of the Doppler frequency shift at the vertical and oblique radiosounding of the ionosphere in the HF range [*Afraimovich et al.,* 1984; *Li et al.,* 1994; *Nagorsky and Taraschuk*, 1992]. The sensitivity of this method in some cases is sufficient for detecting SAW; however, difficulties arise with localization of the formation region of the detected signal, the latter fact being due to the multihop character of HF signal propagation.

[15] The need for information on the time of the event (industrial explosion or earthquake) is the common defect of the above described methods because the disturbance propagation velocity is calculated using the SAW delay relative the event beginning and assuming the constancy of the ve-

locity along the propagation path (which does not always correspond to the reality).

[16] *Afraimovich et al.* [1998, 2001b, 2004] developed a method of determination of the phase velocity and propagation direction of ID using three spatially diverse GPS receivers in the plain front approximation. Unlike the radiophysical methods known earlier, the proposed method provides an estimation of the SAW parameters without a priori information on the place and time of the pulse impact. The period of detected shock-acoustic waves was 180–390 s, and the amplitude exceeded the standard deviation of the background fluctuations of TEC in this range of periods in quiet and moderately disturbed geomagnetic conditions as a minimum by a factor of 2. The elongation angle of the wave vector varied in the limits 20°–44° and the horizontal component of the phase velocity (1100–1300 m $s^{-1}$) was close to the sound speed at heights of the maximum of the ionospheric $F$ region. These data agree to the available ideas on the generation of shock-acoustic waves caused by piston-like motions of the Earth surface in the epicenter zone of the earthquake.

[17] *Afraimovich et al.* [2001a] developed a method of determination of the phase velocity and arrival direction of ID based on the spatial-temporal processing of the TEC variations in the ionosphere on the grating of GPS stations with number higher than three. However, this method is applicable only in the case of a small deviation of the wave front from the plain one. *Afraimovich et al.* [2002a] proposed a method of calculation of ID characteristics (the phase velocity and source location) in the near zone of the earthquake epicenter, that is, when one cannot neglect the spherical character of the wave front.

[18] Both these methods [*Afraimovich et al.*, 2001a, 2002a] are based on the concept of using networks of GPS receivers as a nonequidistant phased antenna grating (PAG) proposed by *Afraimovich* [2000]. The coherent processing of variations in TEC measured simultaneously for all rays at the satellite at all stations of the GPS grating selected for the analysis is based on the known PAG algorithms. Depending on the type of the analyzed disturbance the form of the PAG complex characteristic is chosen corresponding to the spatial-time properties of the given disturbance.

[19] Using GPS gratings in the remote zone of the source in the approximation of the plain front makes it possible to determine the horizontal component of the phase velocity and the direction of the wave vector of the disturbance, but neither the time of switching nor coordinates of the point source. Determination of the coordinates in the horizontal plane becomes possible in this approximation in the regions with a dense network of GPS stations when one can select widely spaced relative to the assumed source various GRS gratings.

[20] In the approximation of a spherical front vice versa the coordinates and the switching-on time may be determined in the near zone of the source; however, a problem of determination of the source height (and so of determination of the phase velocity) appears. Only joint complex use of these approximations proposed in this paper makes it possible to estimate the velocity, coordinates, and switching-on time of the disturbance source.

## 2. Geometry of the Experiment

[21] The earthquake in the vicinity of Hokkaido Island occurred on 25 September 2003 at 1950 UT. Its magnitude was $M = 8.3$. The earthquake epicenter ($\Phi_s = 41.8°$N, $\Lambda_s = 143.85°$E) was located at a depth of 27–33 km under water between the Kurile and Japan cavities. The geometry of the experiment is shown in Figure 1.

[22] The earthquake in the vicinity of Sumatra Island occurred on 4 June 2000 at 1628 UT. The magnitude of the earthquake was 7.7. The epicenter ($\Phi_s = 4.7°$S, $\Lambda_s = 102.1°$E) was located at a depth of 33 km under the Earth surface. The experiment geometry is shown in Figure 2.

[23] The asterisks in Figures 1 and 2 show the position of the epicenter. Crosses correspond to the calculated position of the epicenter. Dark circles and diamonds show locations of the GPS stations and subionospheric points corresponding to the maximum response. The station names and numbers of the PRN satellites are written on Figures 1 and 2.

[24] The above presented information on the earthquakes was taken from the USGS (http://www.usgs.gov/). The coordinates of the GPS stations used in the experiment can be found at the SOPAC Web site (http://sopac.ucsd.edu/).

[25] The level of geomagnetic disturbances during the events in question was quite moderate (the $Dst$ variations were within $-21/11$ nT, the $Kp$ index varied from 1 to 4). The data on the geomagnetic indices $Dst$ and $Kp$ were taken from the WDC site.

[26] The initial data for formation of the spatial-time distribution of the ionospheric responses to SAW are temporal series of the high-frequency variations in TEC $dI(t)$ and corresponding to them series of the azimuth $\alpha(t)$ and elongation angle $\theta(t)$ of the ray to the satellite. The method of data processing was described in detail by *Afraimovich et al.* [2001b].

[27] The time dependences of the initial series of "oblique" TEC $I_i(t)$ for the earthquakes on 4 June 2000 (NTUS; PRN 03) and 25 September 2003 (MIZU; PRN 24) are presented in Figures 3a and 3g, respectively. Figures 3b–3e and 3h–3k show the filtered in the 1–10 min range variations in TEC $dI_i(t)$.

[28] Figure 3 shows that on the background of slow changes in TEC, quick N-shaped oscillations caused by propagation of SAW are distinctly seen. The parameters of the registered responses to the earthquake on 25 September 2003 lie within the following limits: the amplitude and disturbance period change from 0.1 to 0.25 TECU and from 360 to 900 s, respectively (Table 1). The corresponding parameters for the event on 4 June 2000 are from 0.1 to 0.5 TECU and from 180 to 330 s, respectively (Table 2).

[29] To eliminate the uncertainty of the localization of the ionospheric response of SAW caused by the integral character of the TEC values, we assume that the TEC disturbance is formed in the point where the ray to the satellite crosses the plane at a height of $h_d$ above the maximum of the ionospheric $F$ region providing the main input into the TEC formation. Below we take for the calculations a value of $h_d = 400$ km, which in the best way corresponds to the nighttime conditions of the experiment (2328 LT and 0450 LT).

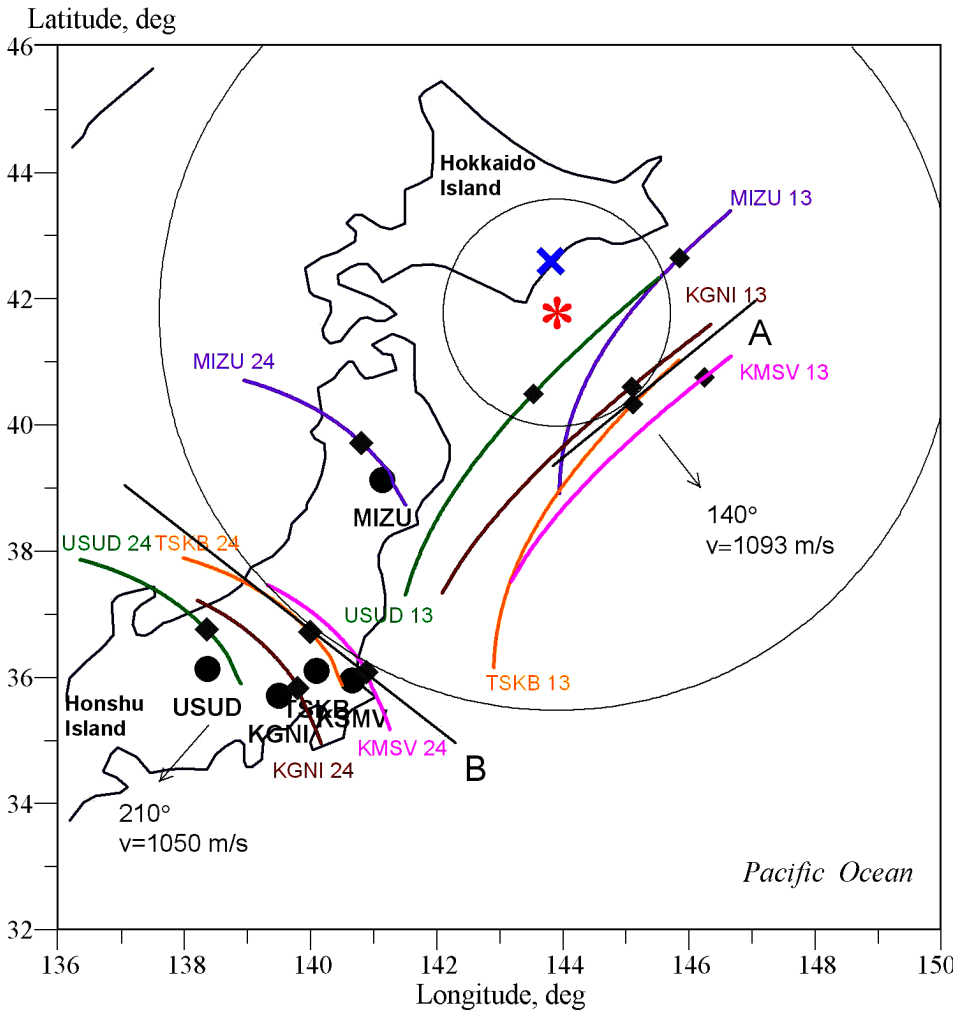


**Figure 1.** The experiment geometry during the 25 September 2003 earthquake in the vicinity of Hokkaido Island (Japan). The dark points and thin curves show the position of the GPS stations and trajectories of subionospheric points, respectively. Diamonds show the positions of subionospheric points in the moments of the maximum deviation of TEC $t_{\min}$. Corresponding numerical data are presented in Table 2. The asterisk and thick cross show the position of the earthquake epicenter and source, respectively. Segments A and B show the fragments of the plain wave front on the circles corresponding to the position of the spherical front of the disturbance at the moments 2000:67 UT and 2000:03 UT. The values of the direction and phase velocity of the wave are written nearby.

The geographical coordinates of the subionospheric point ($\Phi_i$, $\Lambda_i$) were determined for this height. The trajectories of the subionospheric points are shown in Figures 1 and 2 by thin curves. In the scope of our method the TEC disturbances registered at the network of GPS receivers are considered as a set of signals of an nonequidistant phased grating of "ionospheric detectors" with the known coordinates. Calculating the coordinates of subionospheric points for the time moments text, corresponding to the extreme value of the TEC response ($t_{\max}$ for the earthquakes at Sumatra and $t_{\min}$ for the earthquake at Hokkaido are shown in Figures 3c and 3i, respectively), we determine the spatial position of the ionospheric response to SAW. The position of each ray to the satellite is determined by the value of the elongation angle $\theta_s(t)$ counted from the terrestrial surface northward and azimuth $\alpha_s(t)$ counted from the northward direction clockwise for the time moments $t_{\text{ext}}$. Determining the time moments $t_{\text{ext},i}$ for each series $dI_i(t)$ and corresponding co-

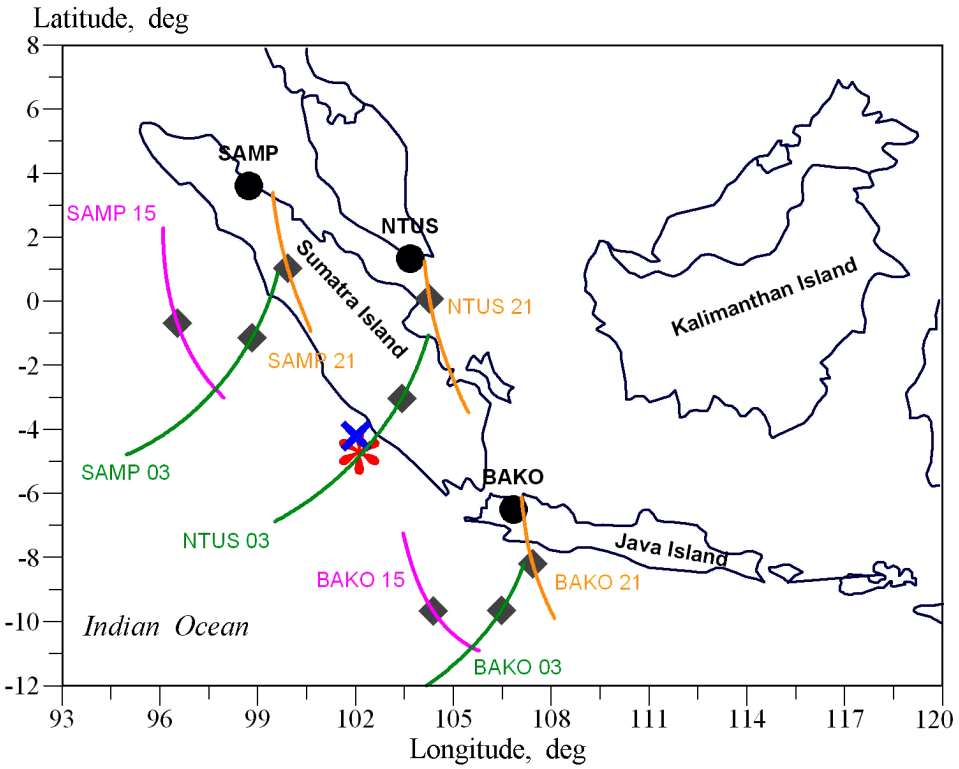


**Figure 2.** Experiment geometry during the 4 June 2000 earthquake near Sumatra Island (Indonesia). The designations are the same as in Figure 1.

ordinates ($\Phi_i$, $\Lambda_i$) of the subionospheric points, we obtain a spatial-time distribution of the ionospheric responses to SAW (Figures 1 and 2). The values of $t_{ext,i}$, $\Phi_i$, and $\Lambda_i$ for each ray "GPS receiver–the satellite" which detected ionospheric responses are shown in Tables 1 and 2.

[30] Figure 4 schematically shows the geometry of the GPS sounding and determination of the parameters of the ionospheric disturbance during the Sumatra earthquake on 4 June 2000. The earthquake epicenter is marked by an asterisk. On top the horizontal cross section of the spherical front of the TEC disturbance propagating with a radial velocity $V$ from the source localized at a height of $h_s = 350 - 400$ km (is marked by a cross) is shown. "Ionospheric detectors" the coordinates of which are determined from the GPS data (diamonds) are detecting the ionospheric response to the disturbance at various moments of time.

**Table 1.** Parameters of the Ionospheric Responses to the Hokkaido Earthquake

| Site-PRN | $t_{min}$, UT | $\Phi_{min}$, ° | $\Lambda_{min}$, ° | $\Delta T$, s | $\delta t$, hours | $V_a$, m s$^{-1}$ |
|---|---|---|---|---|---|---|
| MIZU 13 | 2006:42 | 42.654 | 145.847 | 600 | 0.232 | 428 |
| USUD 13 | 2010:00 | 40.498 | 143.528 | 510 | 0.265 | 352 |
| KSMV 13 | 2011:42 | 40.763 | 146.244 | 360 | 0.282 | 376 |
| TSKB 13 | 2010:48 | 40.337 | 145.112 | 570 | 0.273 | 364 |
| KGNI 13 | 2009:12 | 40.613 | 145.088 | 510 | 0.257 | 374 |
| MIZU 24 | 2015:48 | 39.723 | 140.804 | 417 | 0.323 | 398 |
| USUD 24 | 2030:00 | 36.759 | 138.349 | 871 | 0.465 | 483 |
| KGNI 24 | 2032:30 | 35.832 | 139.795 | 838 | 0.490 | 467 |
| TSKB 24 | 2030:48 | 36.724 | 139.986 | 838 | 0.473 | 431 |
| KSMV 24 | 2030:00 | 36.099 | 140.884 | 748 | 0.465 | 455 |

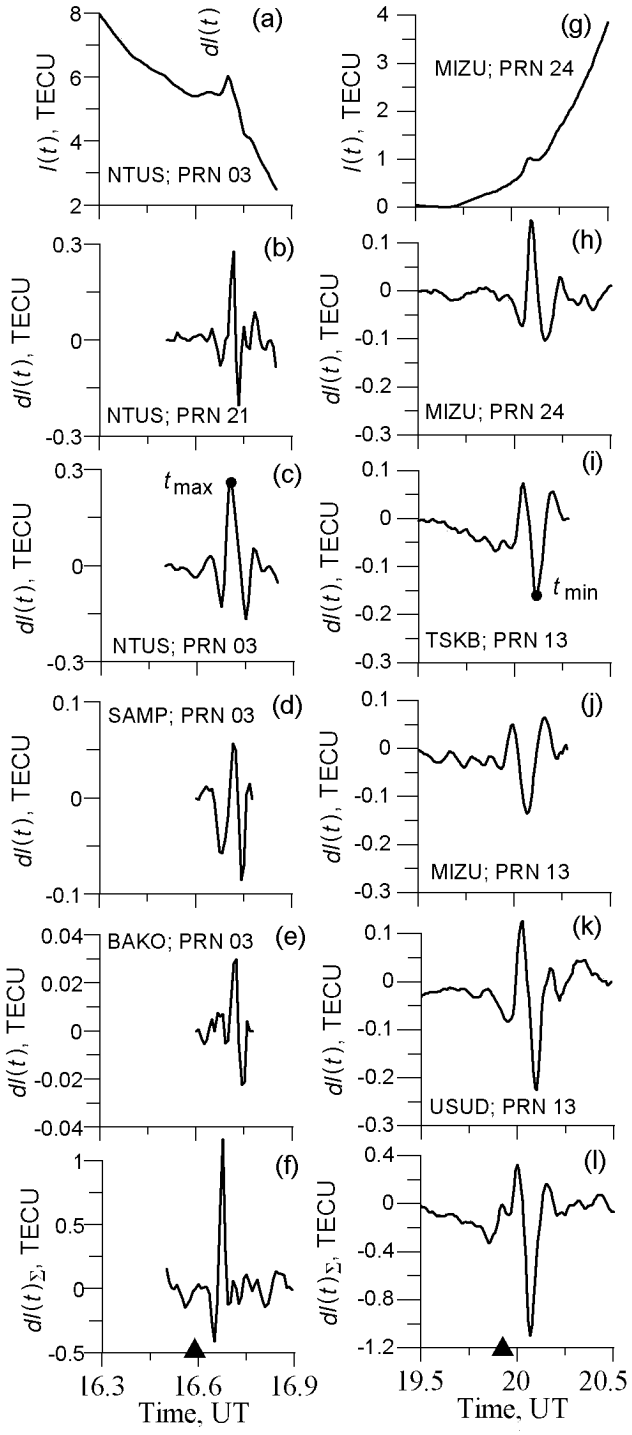


**Figure 3.** Time dependencies of the initial series of the "oblique" TEC $I_i(t)$ for (a) NTUS; PRN 03 and (g) MIZU; PRN 24. (b–e) and (i–k) – filtered out dependencies $dI_i(t)$. (c) and (i) – moments $t_{\max}$ and $t_{\min}$ of the extreme values of the TEC response $dI(t)$. (f) and (l) – signals of the spatial collection $I_\Sigma(t)$ for both events. The solid triangles at the time axis show the moments of the main shock (1628 UT and 1950:07 UT).

## 3. Method of Determination of the "Switch-on Time" and Localization of the Secondary Source of the Ionospheric Disturbance Generated During the Earthquake

[31] Now we consider the complex method proposed by the authors of determination of parameters of the disturbance wave front in the near and remote zones of the source using GPS gratings on the example of the 25 September 2003 earthquake.

[32] The geometry of determination of wave front parameters using GPS gratings in the remote zone of the source is shown in Figure 5. To simplify the calculations, the latitude and longitude of the subionospheric points is recalculated into horizontal Cartesian coordinates $(x_i, y_i)$ in the topocentric coordinate system. The center of the system $(x_0, y_0)$ coincides to the coordinates of the point source of the pulse disturbance. This approximation is true for the distances of the subionospheric points from the epicenter considerably less than the Earth radius, this condition being fulfilled in our case.

[33] The $X$ and $Y$ axes are directed eastward and northward, respectively. The concentric circles show the position of the wave front at various moments of time. The diamonds and symbols $A_1$, $B_1$, and $C_1$ and $A_2$, $B_2$, and $C_2$ denote the GPS stations forming gratings R1 and R2, respectively. $R_0$ and $L$ are radius vectors of points $A_1$ and $C_1$, respectively. The line between points $A_1$ and $C_1$ with a length of $d$ is a base of an elementary interferometer (phase radar) used for determination of the direction (azimuth) of the wave vector $\mathbf{K}$ of the disturbance (the normal to the wave front in the vicinity of points $A_1$ and $C_1$). The azimuths $\alpha_1$ and $\alpha_2$ are marked by dotted arcs.

[34] In the plain front approximation the phase difference $\Delta\varphi$ of the wave disturbance in points $A_1$ and $C_1$ is proportional to sin$\alpha$:

$$\Delta\varphi = \frac{2\pi d}{\lambda}\sin\alpha \tag{1}$$

where $\lambda$ is the wavelength of the disturbance. In the case when vector $\mathbf{K}$ is close to the normal to the position of the base $d$ we write

$$\Delta\varphi \simeq \frac{2\pi d}{\lambda}\alpha \tag{2}$$

In this approximation the error in azimuth calculation $\delta$ is determined by the increment of the phase difference $\sigma(\Delta\varphi)$ proportional to the linear deviation $\delta X$ of the spherical front from the plane front (Figure 5)

$$\delta = \frac{\lambda}{2\pi d}\sigma(\Delta\varphi) = \frac{\delta X}{d} \tag{3}$$

The required accuracy $\delta$ of the azimuth determination depends on the given accuracy of calculation of the coordinates of the source $\Delta R$:

$$\delta = \frac{\Delta R}{R_0} \tag{4}$$

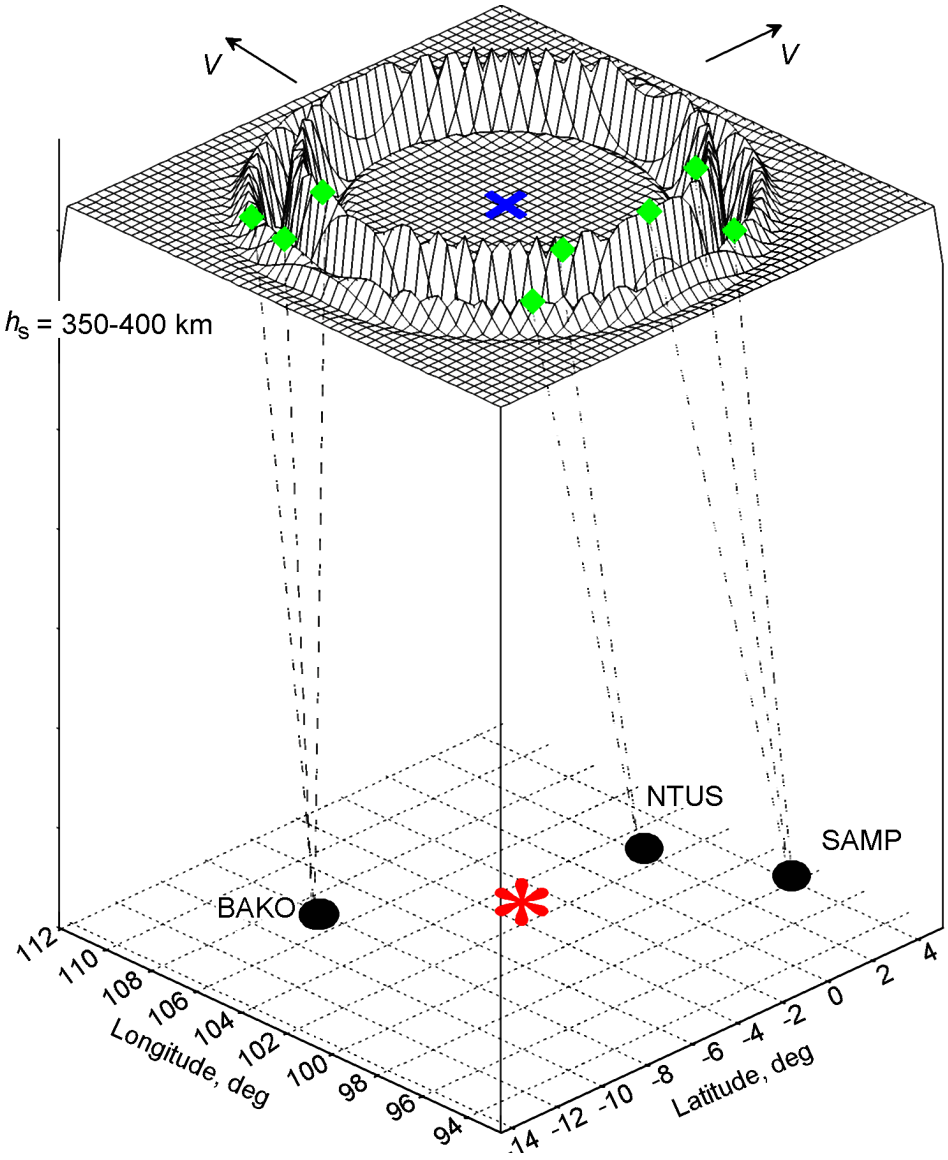


**Figure 4.** Scheme of the GPS sounding during the Sumatra earthquake on 4 June 2000. The earthquake epicenter is shown by the asterisk. A horizontal cross section of the spherical front of the total electron content disturbance propagating with a radial velocity $V$ from the source localized at a height of $h_s$ = 350−400 km (marked by a cross) is shown on the top. The equivalent "ionospheric detectors" (diamonds), the coordinates of which are determined from the GPS data, demonstrate the ionospheric response to the disturbance at various moments of time.

Formulae (4) provides an evaluation of the maximum permitted deviation $\Delta X$

$$\delta X < d\Delta \tag{5}$$

On the other hand, if the base $d$ is small as compared to the distance $R$ to the source ($d^2 \ll R_0^2$) (Figure 5), then

$$\delta X = L - R = \sqrt{R^2 + d^2} - R = R\sqrt{1 + \frac{d^2}{R^2}} - R \approx \frac{d^2}{2R_0} \tag{6}$$

[35] In this case the distance to the remote zone should be larger than

$$R_0 = \frac{d}{2\delta} \tag{7}$$

For the relative accuracy $\delta = 0.05$ and base $d = 100$ km the radius of the remote zone should be $R_0 = 1000$ km. The accuracy of source coordinate determination is in this case ~50 km. The value $R_0 = 1000$ km is close to the dimensions of the aperture of the complete GPS grating of the order of 700 km, i.e., to the maximum dimensions of the spatial distribution of subionospheric points for all GPS stations and

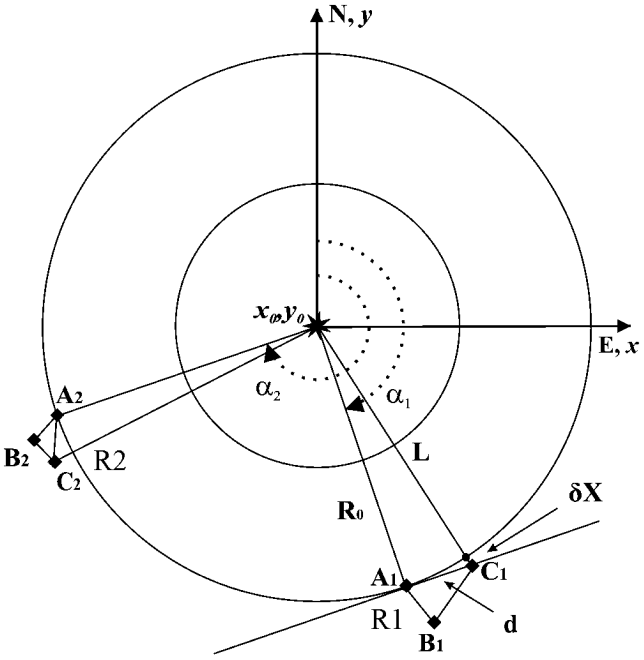


**Figure 5.** Geometry of the determination of the wave front parameters in the near and remote zone of the source using GPS gratings. The concentric circles show the position of the wave front at various moments of time; diamonds and symbols $A_1$, $B_1$, $C_1$ and $A_2$, $B_2$, $C_2$ denote the GPS stations forming the R1 and R2 gratings, respectively; $R_0$ and $L$ are the radius vectors of the $A_1$ and $C_1$ points, respectively. The line between the points $A_1$ and $C_1$ with a length $d$ presents a base of the elementary interferometer used to determine the azimuth of the wave vector **K** of the disturbance. The azimuths $\alpha_1$ and $\alpha_2$ are shown by dotted arcs.

all satellites presented in Figure 1. Thus it follows that particular GPS gratings with the base shorter than 100 km (for example, MIZU, USUD, and TSKB; PRN 13 and USUD, KGNI, and KSMV; PRN 24, see Figure 1) may be used for determination of the direction to the source in the approximation of a plain wave. The presented below evaluations of the disturbance phase velocity in the approximation of a plane front for various combinations of GPS gratings consisting of three stations were obtained using the SADM-GPS method [*Afraimovich et al.,* 1998, 2001b, 2004].

[36] The entire set of the GPS stations presented in Figure 1 is located within the near zone of the source, because for the total aperture of about 700 km at the same requirements to the accuracy of source coordinate determination $\delta = 0.05$ the distance to the remote zone is 7000 km. Therefore for joint processing of the data of the total GPS grating one should use the approximation of the spherical front [*Afraimovich et al.,* 2001a].

[37] We use a simplified model in which the epicenter emitter of SAW during the earthquake is substituted by a point-like source of SAW located at a height of $h_s$ in the ionosphere. At $h_s = 0$ km it coincides to the epicenter of the earthquake. The SAW front presents a sphere expanding from the source in the ionosphere with a constant radial velocity $V_r$. Since only variations of TEC along the "receiver–satellite" ray can be registered at the spatially dispersed GPS detectors, the analysis of the data of GPS gratings makes it possible to evaluate parameters of the wave front only in the horizontal plane. On the other hand, the wavelength of the disturbance is comparable or larger than the scale height of the electron concentration in the $F$ region and the altitude range where AGW still are able to propagate. Therefore in the first approximation the wave front of the secondary disturbance source at the ionospheric level is quite able to be considered as a spherical one.

[38] Moreover, we do not take into account the transformation of the TEC response amplitude to passage of SAW which is determined by the spatial attenuation of the SAW amplitude, aspect relation between the disturbance wave vector, direction to the satellite [*Afraimovich et al.*, 1998, 2004], and orientation of the magnetic field vector [*Afraimovich et al.*, 2001b].

[39] In these conditions the algorithm of spatial-time processing is reduced to summation of the preliminarily phased series $dI_i(t)$ to the reference series $dI_0(t)$. As a result we obtain the total signal of the spatial collection of the TEC series with the remote trend:

$$dI_\Sigma(t) = dI_0(t) + \sum_{i=1}^{M-1} dI_i(t - \Delta\tau_i) \qquad (8)$$

where $\Delta\tau_i$ is the time shift of the $i$th series $dI_i(t)$ relative to

**Table 2.** Parameters of the Ionospheric Responses to the Sumatra Earthquake

| Site-PRN | $t_{\min}$, UT | $\Phi_{\min}$, ° | $\Lambda_{\min}$, ° | $\Delta T$, s | $\delta t$, hours | $V_a$, m s$^{-1}$ |
|---|---|---|---|---|---|---|
| SAMP 03 | 1671:42 | –1.50 | 98.83 | 208 | 0.242 | 690 |
| NTUS 03 | 1670:00 | –3.03 | 103.41 | 331 | 0.225 | 477 |
| BAKO 03 | 1682:30 | –9.45 | 106.59 | 298 | 0.350 | 633 |
| SAMP 15 | 1682:30 | –1.57 | 96.52 | 180 | 0.350 | 625 |
| NTUS 15 | 1665:48 | –3.13 | 100.89 | 270 | 0.183 | 571 |
| BAKO 15 | 1677:30 | –10.06 | 104.36 | 208 | 0.300 | 670 |
| SAMP 21 | 1671:42 | 0.96 | 99.95 | 180 | 0.242 | 864 |
| NTUS 21 | 1671:42 | –0.99 | 104.51 | 237 | 0.242 | 674 |
| BAKO 21 | 1671:42 | –8.31 | 107.47 | 151 | 0.242 | 907 |

the reference series $dI_0(t)$; $i = 1, 2, 3, ..., M$, where $M$ is the number of summated series. The time shift is determined experimentally as a difference of time moments of registration of extremes of SAW responses in the $i$th and background series of TEC with the remote trend:

$$\Delta\tau_i = (t_{\text{ext,i}} - t_{\text{ext},0}) \tag{9}$$

As a reference point we take the position of the ionospheric response to SAW with the minimum value of time $t_{\min}$. For the event on 25 September 2003 the reference point is the subionospheric point MIZU; PRN 13 with the time $t_{\min,0} =$ 20.058 UT. Then the time series of TEC with the remote trend $dI_0(t)$ for the GPS station MIZU; PRN 13 we will also consider as a reference series.

[40] Because of the fact that the TEC oscillation caused by the SAW propagation well mutually correlate in each summated series and the background noise oscillation are not correlated (see Figures 3b, 3c, 3d, 3e, 3h, and 3k), the signal-to-noise ratio in the total signal of the spatial collection increases not less than by a factor of $\sqrt{M}$.

[41] Spatial-time processing of TEC series with remote trend is performed in the scope of the model of the spherical front of the ionospheric disturbance wave propagating from a point source in all directions with a constant radial velocity. According to the accepted model, the time shift of the summated series will be determined by the difference of radial distances of the ionospheric disturbance registration points (subionospheric points) from the acoustic impact source (the earthquake epicenter) as well as by the radial velocity of SAW propagation (Figure 5):

$$\Delta\tau_i = \frac{\Delta\rho_i}{V_r} \tag{10}$$

where $\Delta\rho_i = \rho_i - \rho_0$ is the difference between the radial distances of the $i$th and reference subionospheric points from the ID source and $V_r$ is the radial phase velocity of ID.

[42] Consequently, the expression for the radial distance of the $i$th subionospheric point of the ID source is written as

$$\rho_i = \sqrt{(x_i - x_s)^2 + (y_i - y_s)^2 + (h_d - h_s)^2} \tag{11}$$

where $x_i, y_i$ are the coordinates of the $i$th subionospheric point in the topocentric coordinate system, $h_d$ is a height above the ionization maximum of the ionospheric $F2$ layer (i.e., the height where registration of ID occurs), $x_s, y_s$ are the coordinates of the ID source, and $h_s$ is the assumed height of the ID source.

[43] Bearing in mind that the projection of the reference subionospheric point onto the Earth surface (i.e., $x_0 = 0, y_0 = 0$ is the beginning of the chosen topocentric coordinate system, the expression for the radial distance of the reference subionospheric point from the ID source takes the form

$$\rho_0 = \sqrt{x_s^2 + y_s^2 + (h_d - h_s)^2} \tag{12}$$

Taking into account (11) and (12) the expression (10) is written in the form

$$\Delta\tau_i = [\sqrt{(x_i - x_s)^2 + (y_i - y_s)^2 + (h_d - h_s)^2} - \sqrt{x_s^2 + y_s^2 + (h_d - h_s)^2}]/V_r \tag{13}$$

where $i = 1, 2, 3, ..., M - 1$.

[44] Then for the whole set of ID registration points we obtain the system of $(M - 1)$ equations:

$$\begin{aligned}
\Delta\tau_1 &= [\sqrt{(x_1 - x_s)^2 + (y_1 - y_s)^2 + (h_d - h_s)^2} - \sqrt{x_s^2 + y_s^2 + (h_d - h_s)^2}]/V_r \\
\Delta\tau_2 &= [\sqrt{(x_2 - x_s)^2 + (y_2 - y_s)^2 + (h_d - h_s)^2} - \sqrt{x_s^2 + y_s^2 + (h_d - h_s)^2}]/V_r \\
&\dots \\
\Delta\tau_{M-1} &= [\sqrt{(x_{M-1} - x_s)^2 + (y_{M-1} - y_s)^2 + (h_d - h_s)^2} - \sqrt{x_s^2 + y_s^2 + (h_d - h_s)^2}]/V_r
\end{aligned} \tag{14}$$

[45] An approximate solution of the obtained system relative to $x_s, y_s, V_r$ is found numerically by the random search method under the condition of minimum of the mean square discrepancies $\sigma_t$ of the left-hand and right-hand sides of the equations. The range of looking for the value of each searched parameter and the step of its change are prescribed. For the sake of convenience in the work, the range and step for looking of the ID source location are prescribed in geographical coordinates $\Lambda_s$, and $\Phi_s$, which are transformed into topocentric coordinates in the process of calculation.

[46] In the search process an exhaust of all possible values of $\Lambda_s$, $\Phi_s$, and $V_r$ in the given range and with the given step is performed and for each combination of these parameters a value of the mean square of discrepancies $\sigma_t$ is determined. The values of $\Lambda_s$, $\Phi_s$, and $V_r$, providing the minimum value of $\sigma_t$, are taken as a solution of the equation system and therefore the ID parameters looked for.

[47] The calculation of the "switch-on time" of the ID source is performed in the scope of the accepted model of the spherical front on the basis of the calculated source coordinates $\Lambda_s$, and $\Phi_s$ and phase radial velocity $V_r$ taking into account the known time of the registration of the SAW response in the reference point $t\min, 0$. In this case the expression for determination of the "switch-on time" of the ID source is written in the following form:

$$t_s = t_{\min,0} - \frac{\rho_0}{V_r} \tag{15}$$

where $\rho_0$ is the radial distance of the reference subionospheric point from the calculated position of the ID source.

[48] The form of the signal of the spatial collection $dI_\Sigma(t)$ is an indirect criterion of correct solution of the equation

**Table 3.** Spatial-Time Characteristics of the Ionospheric Response to the Hokkaido Earthquake on 25 September 2003

| $h_s$, km | $\Phi_s$, ° E | $\Lambda_s$, ° N | $t_s$, UT | $\delta t$, s | $V_r$, m s$^{-1}$ | $V_v$, m s$^{-1}$ |
|---|---|---|---|---|---|---|
| 400 | 42.6 | 143.8 | 2000.0 | 594 | 700 | 673 |
| 300 | 42.8 | 143.8 | 1998.9 | 554 | 700 | 541 |
| 200 | 43.0 | 143.6 | 1995.0 | 414 | 650 | 483 |
| 100 | 43.0 | 143.0 | 1990.7 | 259 | 600 | 386 |
| 0 | 43.2 | 143.6 | 1984.2 | 25 | 550 | – |
| – | 41.8 | 143.85 | 1983.5 | | | |

system (12). Such signal for the 25 September 2003 event is shown in Figure 3l. One can see that the amplitude of the summated signal exceeds the amplitude of the reference signal $dI_\Sigma(t)$ for the path MIZU; PRN 13 (Figure 3i) almost by an order of magnitude, which corresponds to the total number of paths. Moreover, the TEC variations outside the response are considerably lower then for individual paths, the fact manifesting an increase of the signal-to-noise ratio. The signal of the spatial collection $dI_\Sigma(t)$ for the 4 July 2000 event is shown in Figure 3f.

[49] It should be noted that the accuracy in determination of the phase velocity $V$ in the approximation of the plain front is considerably higher than under using the algorithm for the spherical front. In the former case for each GPS station the detection of the disturbance is performed for the same satellite with the same aspect conditions and the velocity of the shift of the reference system, so one has only to take into account this shift in the scope of the SADM-GPS method [*Afraimovich et al.*, 1998, 2004]. In the latter case solution of the equation system (12) is performed relative to the rays to different satellites with different aspect conditions and shift velocities of different reference systems not taken into account in the described method in the first approximation. Though the reference system shift (up to 50 m s$^{-1}$ at a height of 400 km at the elongation angles above 30°) occurs with velocities much slower than the phase velocity $V$ of the wave (1000 m s$^{-1}$) this error may be only by several times less than the value of $V$ itself. In future a modernization of the method in the approximation of the spherical front is needed taking into account corresponding aspect conditions and shifts of the reference systems for each ray to the satellite.

## 4. Experimental Results

[50] Using formulae (8)–(12) in the approximation of the spherical disturbance front for the events on 25 September 2003 and 4 June 2000 the values of the coordinates $\Phi_s$ and $\Lambda_s$, time moment $t_s$, and the delay $\delta_t$ of the ID source switching relative to the moment of the main shock $t_0$, and also of the radial velocity $V_r$ of the ID motion and spatial discrepancy $\sigma$ for various values of the height $h_s$ of the assumed ID source were calculated (Tables 1 and 2).

[51] Besides these values, the mean value of the vertical velocity $V_v$ of propagation of acoustic disturbance from the epicenter to the secondary source in the ionosphere was calculated using the simple relation

$$V_v = \frac{h_s}{\delta t} \tag{16}$$

One can easily see that at the radial velocity $V_r$ of the disturbance propagation of the order of 700 m s$^{-1}$ the calculated moment of switching on of the ionospheric disturbance source for the 25 September 2003 earthquake is late relative to the main shock by 10 min (Table 3). This fact agrees to the concept that the secondary source of the ionospheric disturbance is located in the ionosphere at a height of the order of 300–400 km.

[52] Similar situation takes place for the calculated characteristics of ID during the 4 June 2000 earthquake. Table 4 shows that the secondary disturbance source at a height of 300–400 km switches on 7–8 min after the main shock, the radial velocity of disturbance propagation being 1000–1050 m s$^{-1}$. The mean value of the vertical velocity $V_v$ of

**Table 4.** Spatial-Time Characteristics of the Ionospheric Response to the Sumatra Earthquake on 4 June 2003

| $h_s$, km | $\Phi_s$, ° E | $\Lambda_s$, ° N | $t_s$, UT | $\delta t$, s | $V_r$, m s$^{-1}$ | $V_v$, m s$^{-1}$ |
|---|---|---|---|---|---|---|
| 400 | –4.2 | 102.0 | 1661.18 | 496 | 1050 | 806 |
| 300 | –4.2 | 102.0 | 1660.18 | 460 | 1000 | 652 |
| 200 | –4.0 | 102.2 | 1657.36 | 364 | 900 | 549 |
| 100 | –4.0 | 102.0 | 1654.42 | 261 | 850 | 383 |
| 0 | –4.0 | 102.0 | 1649.54 | 86 | 750 | – |
| – | 4.72 | 102.1 | 1647.30 | | | |

propagation of the acoustic disturbance from the epicenter to the secondary source was found close to the mean value of the speed of sound in the height range from the ground to $h_s$ (see the vertical profile of the speed of sound in Figure 6 from *Li et al.* [1994]).

[53] The coordinates of the ID source calculated with an accuracy of 50–60 km agree well with the position of the earthquake epicenter. The difference between the obtained and true (determined from seismic data) values may be explained by the fact that an approximation of the plain Earth was used in the method. This approximation gives corresponding deviation at a distance of about 500 km.

[54] Moreover, the presence of the meridional and zonal winds at ionospheric heights leads to a shift and deformation of the wave front and, respectively, to appearance of the dependence of the acoustic wave intensity on the propagation direction. Here the deciding role is played by the wind velocity gradient [*Ahmadov and Kunitsyn*, 2003, 2004; *Li et al.*, 1994]. This can explain the shift of the horizontal position of the secondary disturbance source in the ionosphere relative to the earthquake epicenter.

[55] The phase velocity of the ID motion at the height $h_d$ may be more precisely determined in the approximation of the plain front for groups of subionospheric points if the distance between these points satisfies the approximation of the plain wave (Figure 5). In our experiment such approximation is fulfilled for ID generated during the Hokkaido earthquake. For the nearest to the epicenter set of subionospheric points (MIZU, USUD, TSKB; PRN 13) located to the southeast from the epicenter (marked by letter A in Figure 1), the direction $\alpha$ of the propagation wave vector and phase velocity were found 140° and $V_h = 1093$ m s$^{-1}$, respectively. For the more distant GPS grating (USUD, KGNI, KSMV; PRN 24) located to the southwest from the epicenter (marked by a letter B in Figure 1), the value of the phase velocity $V_h = 1050$ m s$^{-1}$ almost did not change; however, the direction angle was found equal to $\alpha = 210°$. In Figure 1 the segments A and B mark fragments of the plain wave front on the circles corresponding to the position of the spherical front of the disturbance at the moments 2000:067 UT and 2003 UT. Adjacent to them the values of the direction and phase velocity of the wave are written.

[56] The value of $V_h$ determined in such a way makes it possible to chose between various values of the height $h_s$ of the assumed source of the ID spherical wave presented in Table 3. The value $V_r = 700$ m s$^{-1}$ for the source at a height of $h_s = 400$ km is the closest value of $V_h$ for the 25 September 2003 event. The difference between these velocities may be explained by the fact that the Earth spherical form and different geometry of the rays to the PRN 13 and PRN 24 satellites [*Afraimovich et al.,* 1998] are not taken into account in the used procession method [*Afraimovich et al.*, 2002a].

## 5. Discussion and Conclusions

[57] It should be noted that the calculated phase velocity (about 1000 m s$^{-1}$) for the height $h_s = h_d$ is close to the velocity determined in the approximation of the plain front and to the speed of sound at heights of the electron concentration maximum in the ionosphere. (Figure 6) [*Li et al.*, 1994].

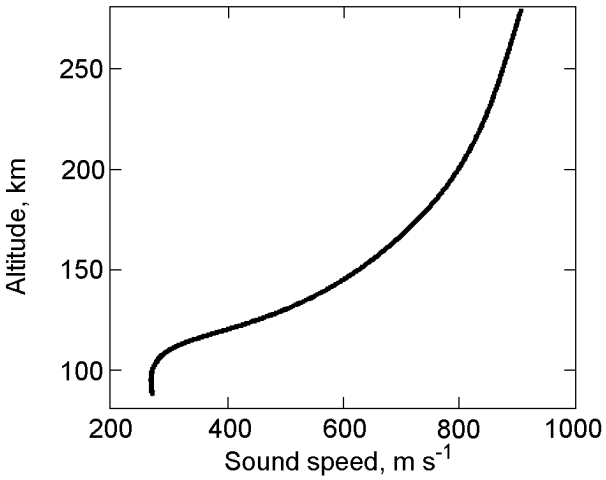


**Figure 6.** Vertical profile of the speed of sound in the linear-acoustic model [*Li et al.*, 1994].

[58] It is worth comparing the results of the spatial-time processing in the approximation of the spherical front (Tables 3 and 4) to the estimates of the mean velocity of the SAW propagation $V_a$ determined from the delay $\Delta_t = t_{\text{ext}} - t_0$ and known length of the path between the earthquake epicenter and subionospheric point. The path length is determined along the great circle arc. The velocity value obtained in such a way varies within 352–483 m s$^{-1}$ and 477–907 m s$^{-1}$ for ID on 25 September 2003 and 4 June 2000, respectively. On the average it is by a factor of 1.5 less than the value of $V_r$ in Tables 3 and 4.

[59] The difference is easily explained by the fact that the path length $L$ is determined along the Earth surface whereas the detecting is conducted in the vicinity of the main electron concentration maximum at a height of 400 km, making the path longer in our case by a factor of 1.5.

[60] Thus the method of determination of the phase velocity $V_a$ used earlier [*Calais and Minster*, 1995] was giving wrong (underestimated) evaluations of the disturbance propagation velocity. This method did not take into account rather complicated propagation mechanism discussed in this paper. In this mechanism at the first stage the acoustic disturbance propagates within a narrow cone of the zenith angles up to ionospheric heights and then in the form of a spherical wave diverges with the radial velocity close to the speed of sound at these heights.

[61] In this section the values of the phase velocity obtained of about 1000 m s$^{-1}$ agree to the data of other experiments on determination of the ID velocity during earthquakes [*Afraimovich et al.*, 2001a, 2001b, 2002a, 2002b]. These data are compiled into Table 5.

[62] Thus it is found that the ionospheric disturbances generated in the moment of the main shock during the 4 June 2000 and 25 September 2003 earthquakes have a form of a spherical wave diverging with a velocity of about 1000 m s$^{-1}$

**Table 5.** Velocity of the Ionospheric Disturbance Propagation During the Earthquakes of 1999–2003 Determined in the Approximation of the Spherical and Plain Fronts

| Date | Day | Epicenter | $M$ | $t_0$, UT | Depth, km | $V_h$, m s$^{-1}$ |
|---|---|---|---|---|---|---|
| | | | Plain Front | | | |
| 17 Aug 1999 | 229 | 40.75°N, 29.86°E | 7.6 | 0001:39 | 17 | 1286 |
| 12 Nov 1999 | 316 | 40.76°N, 31.16°E | 7.2 | 1657:19 | 10 | 1478 |
| 25 Sep 2003 | 268 | 41.78°N, 143.90°E | 8.3 | 1950:06 | 27 | A 1093 B1050 |
| | | | Spherical Front | | | |
| 4 Jun 2000 | 156 | 4.72°S, 102.09°E | 7.9 | 1628:26 | 33 | 900 |
| 25 Sep 2003 | 268 | 41.78°N, 143.90°E | 8.3 | 1950:06 | 27 | 700 |

from the "secondary source" located over the epicenter at the level of the ionospheric $F2$ layer (300–400 km), the "switching on" of the source being delayed relative the moment of the main seismic shock by ∼10 min. The results agree with theoretical models according to which the atmospheric disturbance propagates within a narrow cone of zenith angles up to ionospheric heights and then diverges in the form of a spherical wave with the radial velocity close to the speed of sound at these heights.

[63] **Acknowledgments.** The authors thank A. M. Uralov and V. V. Evstafiev for their interest in the study and useful discussion and also S. V. Voeikov for his help in processing of the initial data. The work was supported by the Russian Foundation for Basic Research (project 03-05-64100) and also by the grant N 272.2003.5 of the State Support of the Leading Scientific Schools of the Russian Federation. We thank the staff of the Scripps Orbit and Permanent Array Center (SOPAC) for providing us with the used in this paper initial data of the global network of ground-based two-frequency GPS receivers.

## References

Afraimovich, E. L. (2000), The GPS global detection of the ionospheric response to solar flares, *Radio Sci., 35,* 1417.

Afraimovich, E. L., I. I. Varshavsky, B. O. Vugmeister, and A. D. Kalikman (1984), Impact of ground-based industrial explosions on the Doppler and angular characteristics of the signal reflected from the ionosphere, *Geomagn. Aeron* (in Russian), *24*(2), 322.

Afraimovich, E. L., K. S. Palamartchouk, and N. P. Perevalova (1998), GPS radio interferometry of traveling ionospheric disturbances, *J. Atmos. Terr. Phys., 60*(12), 1205.

Afraimovich, E. L., V. V. Chernukhov, and V. V. Kirushkin (2001a), Spatial-time characteristics of the ionospheric disturbance caused by shock-acoustic waves generated by rocket launches, *Radiotech. Electr.* (in Russian), *46*(11), 1299.

Afraimovich, E. L., N. P. Perevalova, A. V. Plotnikov, and A. M. Uralov (2001b), The shock-acoustic waves generated by the earthquakes, *Ann. Geophys., 19,* 395.

Afraimovich, E. L., V. V. Kirushkin, and N. P. Perevalova (2002a), Determination of the characteristics of ionospheric disturbance in the near zone of the earthquake epicenter, *Radiotech. Electr.* (in Russian), *47*(7), 822.

Afraimovich, E. L., E. A. Kosogorov, and A. V. Plotnikov (2002b), Shock-acoustic waves generated at rocket launches and earthquakes, *Space Res.* (in Russian), *40*(3), 261.

Afraimovich, E. L., E. I. Astafieva, and S. V. Voyeikov (2004), Isolated ionospheric disturbances as deduced from global GPS network, *Ann. Geophys., 22,* 47.

Ahmadov, R. R., and V. E. Kunitsyn (2003), Numerical method of solution of the problem of propagation of acoustic-gravity waves in the atmosphere up to ionospheric heights, *Proc. Moscow Univ., Phys. Astron.* (in Russian), *Ser. 3*(3), 38.

Ahmadov, R. R., and V. E. Kunitsyn (2004), Modeling of ionospheric disturbances caused by earthquakes and explosions, *Geomagn. Aeron.* (in Russian), *44*(1), 105.

Andreeva, E. S., M. B. Gokhberg, V. E. Kunitsyn, E. D. Tereshchenko, B. Z. Khuducon, and S. L. Shalimov (2001), Radiotomograthy registration of ionospheric disturbances from the ground-based explosions, *Space Res.* (in Russian), *39*(1), 13.

Barry, G. H., L. J. Griffiths, and J. C. Taenzer (1966), HF radio measurements of high-altitude acoustic-waves from a ground level explosion, *J. Geophys. Res., 71,* 4173.

Blanc, E., and A. R. Jacobson (1989), Observation of ionospheric disturbances following a 5-kt chemical explosion: 2. Prolonged anomalies and stratifications in the lower thermosphere after shock passage, *Radio Sci., 24,* 739.

Calais, E., and J. B. Minster (1995), GPS detection of ionospheric perturbations following the January 1994, Northridge earthquake, *Geophys. Res. Lett., 22,* 1045.

Calais, E., J. B. Minster, M. A. Hofton, and M. A. H. Hedlin (1998), Ionospheric signature of surface mine blasts from Global Positioning System measurements, *Geophys. J. Int., 132,* 191.

Fitzgerald, T. J. (1997), Observations of total electron content perturbations in GPS signals caused by a ground level explosion, *J. Atmos. Terr. Phys., 59,* 829.

Francis, S. N. (1975), Global propagation of atmospheric gravity waves: A review, *J. Atmos. Terr. Phys., 37,* 1011.

Golitsyn, G. S., and V. I. Klyatskin (1967), Oscillations in the atmosphere caused by motions of the Earth surface, *Phys Atmos. Ocean* (in Russian), *111*(10), 1044.

Li, Y. Q., A. R. Jacobson, R. C. Carlos, R. S. Massey, Y. N. Taranenko, and G. Wu (1994), The blast wave of the shuttle plume at ionospheric heights, *Geophys. Res. Lett., 21,* 2737.

Massey, R. S., R. C. Carlos, A. R. Jacobson, and G. Wu (1994), Observations of TEC fluctuations from an explosion on the earth's surface, in *Proceedings of the International Beacon Satellite Symposium, edited by L. Kersley,* p. 128, Univ. of Wales, Aberystwyth, U.K.

Nagorsky, P. M. (1985), Disturbances of the electron concentration in the ionosphere caused by ground-based explosions, *Phys. Earth* (in Russian), *11,* 66.

Nagorsky, P. M., and Yu. E. Taraschuk (1992), Ionospheric disturbances caused by powerful explosions, *Physics* (in Russian), *35,* 110.

Orlov, V. V., and A. M. Uralov (1984), Reaction of the atmosphere to a weak ground-based explosion, *Phys. Atmos. Ocean* (in Russian), *20*(6), 476.

Pavlov, V. A. (1979), Impact of earthquakes and volcano erup-

tions on the ionospheric plasma, *Radiophysics* (in Russian), *22,* 19.

Pavlov, V. A. (1986), Acoustical pulse over the earthquake epicenter, *Geomagn. Aeron.* (in Russian), *26*(5), 807.

Rodionov, V. N., V. V. Adushkin, and V. N. Kostyushenko (1971), *Mechanical Effects of Underground Explosions edited by M. A. Sadovsky* (in Russian), Nedra, Moscow.

Row, R. V. (1967), Acoustic-gravity waves in the upper atmosphere due to a nuclear detonation and an earthquake, *J. Geophys. Res., 72,* 1599.

Rudenko, G. V., and A. M. Uralov (1995), Calculation of ionospheric effects due to acoustic radiation from an underground nuclear explosion, *J. Atmos. Terr. Phys., 57*(3), 225.

Uizem, G. (1977), *Linear and Nonlinear Waves* (in Russian), 622 pp., Mir, Moscow.

---

E. L. Afraimovich, E. I. Astafieva, and V. V. Kirushkin, Institute of Solar-Terrestrial Physics, Post Box 4026, Irkutsk 664033, Russia. (afra@iszf.irk.ru)